JOURNAL OF VIROLOGY, Aug. 2010, p. 7634–7641 Vol. 84, No. 15
0022-538X/10/$12.00 doi:10.1128/JVI.02576-09

Tyrosine Residues in the Cytoplasmic Domains Affect Sorting and Fusion Activity of the Nipah Virus Glycoproteins in Polarized Epithelial Cells[▽]

Carolin Weise, Stephanie Erbar, Boris Lamp, Carola Vogt,† Sandra Diederich,‡ and Andrea Maisner*

Institute of Virology, Philipps University of Marburg, D-35043 Marburg, Germany

Received 9 December 2009/Accepted 6 May 2010

The highly pathogenic Nipah virus (NiV) is aerially transmitted and causes a systemic infection after entering the respiratory tract. Airway epithelia are thus important targets in primary infection. Furthermore, virus replication in the mucosal surfaces of the respiratory or urinary tract in later phases of infection is essential for virus shedding and transmission. So far, the mechanisms of NiV replication in epithelial cells are poorly elucidated. In the present study, we provide evidence that bipolar targeting of the two NiV surface glycoproteins G and F is of biological importance for fusion in polarized epithelia. We demonstrate that infection of polarized cells induces focus formation, with both glycoproteins located at lateral membranes of infected cells adjacent to uninfected cells. Supporting the idea of a direct spread of infection via lateral cell-to-cell fusion, we could identify basolateral targeting signals in the cytoplasmic domains of both NiV glycoproteins. Tyrosine 525 in the F protein is part of an endocytosis signal and is also responsible for basolateral sorting. Surprisingly, we identified a dityrosine motif at position 28/29 in the G protein, which mediates polarized targeting. A dileucine motif predicted to function as sorting signal is not involved. Mutation of the targeting signal in one of the NiV glycoproteins prevented the fusion of polarized cells, suggesting that basolateral or bipolar F and G expression facilitates the spread of NiV within epithelial cell monolayers, thereby contributing to efficient virus spread in mucosal surfaces in early and late phases of infection.

Nipah virus (NiV) is a zoonotic and highly pathogenic member of the genus *Henipavirus* within the family *Paramyxoviridae*. NiV emerged for the first time in 1998 and caused an outbreak of respiratory disease in pigs and fatal encephalitis in humans in Malaysia and Singapore (9). Fruit bats of the genus *Pteropus* have been identified as the major natural reservoir host (50). Due to the lack of therapeutic or prophylactic options and the high mortality rates associated with human infections, work with live NiV requires biosafety level 4 (BSL-4) containment.

As a typical member of the family *Paramyxoviridae*, NiV possesses two viral surface glycoproteins that are required for virus entry and spread. Glycoprotein G is responsible for the binding of the virus to cellular ephrin-B2 and -B3 receptors (3, 35, 36). After receptor binding, the viral fusion protein F mediates pH-independent fusion of viral and cellular membranes (virus entry) or fusion of cellular membranes (cell-to-cell fusion). To be fusion active, the precursor F_0 must be proteolytically cleaved into the subunits F_1 and F_2 by host cell proteases. This proteolytic activation requires clathrin-mediated endocytosis, due to a tyrosine-based signal in the cytoplasmic tail of the F protein, and subsequent cleavage by endosomal cathepsin L (12, 37, 45). Only after recycling from endosomes to the cell surface is fusion-active F protein available for incorporation into budding virions or for the initiation of cell-to-cell fusion (13).

The respiratory tract is the most common route of virus entry into the human body. Following respiratory invasion, some viruses, such as influenza virus and severe acute respiratory syndrome (SARS) coronavirus, remain localized, and virions are disseminated only locally by transport in mucus or inflammatory exudates, which permit access to new target cells in the lung. Even if these viruses can cause severe diseases, they fail to penetrate beyond the mucosal surface. Other viruses, such as measles, mumps, rubella, and varicella viruses, also infect via the respiratory tract but then enter the blood circulation from the airways without causing major local symptoms. NiV enters via the airways and subsequently spreads systemically, with extensive endothelial involvement leading to vasculitis, which is mostly responsible for the clinical disease. In addition, NiV often causes symptomatic respiratory infections. Respiratory illness is generally observed in pigs and in about half of human infections (9, 24, 30, 38). A retrospective analysis of NiV outbreaks in Bangladesh strongly suggested that the patients with symptomatic respiratory tract infections were responsible for human-to-human transmission (24). Thus, NiV infection of the airway mucosa is relevant not only for primary NiV infection, serving as a portal of virus entry, but also for virus shedding and transmission to other hosts. Beside respiratory epithelia, epithelial cells in the kidney and bladder have been shown to be infected *in vivo* and are suggested to be important sites of release of progeny virions into the urine (8, 29, 34, 49; for a review, see reference 26).

The major characteristics of polarized epithelial cells are structurally and functionally discrete apical and basolateral plasma membrane domains. To maintain the distinct protein

* Corresponding author. Mailing address: Institute of Virology, Hans-Meerwein-Str. 2, 35043 Marburg, Germany. Phone: 49 6421 2865360. Fax: 49 6421 2868962. E-mail: maisner@staff.uni-marburg.de.

† Present address: German Research Foundation (DFG), Kennedyallee 40, 53175 Bonn, Germany.

‡ Present address: Department of Microbiology and Immunology, Life Science Centre, University of British Columbia, 3559-2350 Health Science Mall, Vancouver V6T 1Z3, British Columbia, Canada.

▽ Published ahead of print on 19 May 2010.

compositions of these domains, newly synthesized membrane proteins must be sorted to their sites of ultimate function and residence (28). Due to the polarized nature of epithelia, virus receptors or viral proteins can be selectively expressed at either apical or basolateral cell surfaces. This can restrict virus entry, budding, or cell-to-cell fusion, with significant implications for virus spread and thus for pathogenesis. The aim of this study was to elucidate the molecular mechanisms of NiV spread within epithelial cells, focusing on the roles of the two surface glycoproteins G and F. We could show that infection of polarized MDCK cells leads to the formation of viral foci. The finding that both NiV glycoproteins not only were expressed apically but also were present at lateral membranes in infected cells adjacent to noninfected cells suggested that the infection spreads by cell-to-cell fusion. When we analyzed the distributions of F and G proteins upon single expression, we observed that the presence of the glycoproteins at (baso)lateral membranes is signal mediated. We could demonstrate that both proteins possess tyrosine-based targeting motifs in their cytoplasmic tails (Y_{525} in the F protein and $Y_{28/29}$ in the G protein), which mediate sorting to the basolateral membranes of polarized epithelia. Fusion of polarized cells was observed only when the basolateral sorting signals of both glycoproteins were intact. These observations support the notion that basolateral or bipolar expression of F and G proteins is required and responsible for the spread of infection across the lateral junctions via glycoprotein-mediated cell-to-cell fusion.

MATERIALS AND METHODS

Cell culture and virus infection. Madin-Darby canine kidney (MDCK) cells were grown in Eagle's minimal essential medium (MEM; Gibco) containing 10% fetal calf serum (FCS), 100 U of penicillin/ml, and 0.1 mg of streptomycin/ml. For polarized growth, cells were seeded on 0.4-μm-pore-size filter supports (ThinCerts tissue culture inserts; Greiner Bio-One). To monitor cell polarization, the transepithelial resistance (TER) was controlled daily using a Millipore-ERS apparatus. Analyses were performed only with cells that gave TER values above 200 Ω per cm^2.

The NiV strain used in this study was isolated from a human brain (kindly provided by J. Cardosa) and was propagated as described previously (31). For NiV infection studies, MDCK cells were grown for 5 days on filter supports with daily medium changes until they had developed a fully polarized phenotype. Cells were then infected by addition of 5×10^7 50% tissue culture infectious doses ($TCID_{50}$) of NiV to the apical filter chamber for 1.5 h at 37°C. Unbound virus was removed by extensive washings, and cells were cultured with Dulbecco's modified Eagle medium (DMEM; (Gibco) with 2% FCS at 37°C. All work with live NiV was performed under BSL-4 conditions.

Virus growth and syncytium formation. MDCK cells were grown on ThinCerts filter supports and were infected with NiV. At different time points postinfection (p.i.), virus titers in the apical supernatants were determined by the $TCID_{50}$ method on Vero cells. Syncytium formation was visualized by indirect immunofluorescence. After permeabilization with methanol-acetone (1:1) and fixation with 4% paraformaldehyde (PFA) for 48 h, cells were incubated with a polyclonal antiserum from infected guinea pigs (gp3; kindly provided by Heinz Feldmann) at a dilution of 1:1,000 for 1 h at 4°C. Primary antibodies were then detected with Alexa Fluor 568-conjugated secondary antibodies (dilution, 1:250). Samples were mounted in Mowiol 4-88 and were analyzed using a Zeiss Axiovert 200M microscope.

Plasmid constructs and stable expression in MDCK cells. cDNA fragments spanning the F and the G genes of the NiV genome (GenBank accession number AF212302) were cloned into the pczCFG5 vector (31). The F and G mutants were generated by introducing site-specific mutations into the double-stranded pczCFG5 plasmids by using a QuikChange mutagenesis kit (Stratagene) as described previously (31). By using complementary oligonucleotide primers, tyrosine or leucine residues in the cytoplasmic tails of F and G were changed to alanine to generate the F_{Y525A}, $F_{Y542/543A}$, $G_{Y28/29A}$, and $G_{L41/42A}$ mutants (45) (see Fig. 5A). For stable expression of wild-type (wt) and mutant F or G proteins, MDCK cells were transfected with the expression plasmids using the transfection reagent Lipofectamine 2000 (Life Technologies, Inc.). Cells were selected for pczCFG5-encoded zeocin resistance by addition of 1.0 mg of zeocin (InvivoGen) per ml of medium. Selected cell clones were screened for stable expression of F and G proteins by immunofluorescence analysis.

Surface immunofluorescence analysis of polarized MDCK cells. MDCK cells were grown on filter supports and were infected with NiV. At 18 or 24 h p.i., NiV-infected cells were fixed with 4% PFA in DMEM for 48 h; then they were incubated from both sides with the polyclonal antiserum from infected guinea pigs (gp3) or with rabbit monoclonal antibodies directed against the NiV F or the NiV G protein (mab92 or mab26, respectively; kindly provided by Benhur Lee) for 2 h at 4°C. The primary antibodies were detected using Alexa Fluor 568-conjugated secondary antibodies (Invitrogen) for 1.5 h at 4°C. To visualize cell junctions, cells were permeabilized for 5 min with methanol-acetone (1:1) and were stained with a monoclonal antibody against E-cadherin (BD Biosciences Pharmingen) and Alexa Fluor 488-conjugated secondary antibodies (Invitrogen). Filters were cut out from their supports, mounted onto microscope slides in Mowiol 4-88 (Calbiochem), and analyzed using a Zeiss Axiovert 200M microscope or a confocal laser scanning microscope (LSM510; Zeiss). MDCK cells stably expressing wild-type or mutant F or G proteins were grown on filter supports and were incubated with the polyclonal anti-NiV serum gp3 for 2 h at 4°C without prior fixation. Primary antibodies were visualized using Alexa Fluor 568-labeled secondary antibodies for 1.5 h at 4°C. Confocal fluorescence images were recorded with a Zeiss LSM510 or a Leica SP5 microscope.

Selective surface biotinylation and immunoprecipitation. MDCK cells stably expressing either F or G proteins were grown on filter supports. Seven days after seeding, selective surface biotinylation was performed as described recently (41). Briefly, cells were incubated twice for 20 min each time at 4°C with 2 mg/ml sulfo-*N*-hydroxysuccinimidobiotin (S-NHS biotin; Pierce) at either the apical or the basolateral surface. After biotinylation, cells were washed with cold phosphate-buffered saline (PBS) containing 0.1 M glycine and were lysed in 0.5 ml of radioimmunoprecipitation assay buffer (1% Triton X-100, 1% sodium deoxycholate, 0.1% sodium dodecyl sulfate [SDS], 0.15 M NaCl, 10 mM EDTA, 10 mM iodoacetamide, 1 mM phenylmethylsulfonyl fluoride, 50 U/ml aprotinin, and 20 mM Tris-HCl [pH 8.5]). After centrifugation for 45 min at 19,000 × *g*, 0.5% of the supernatants was used directly for SDS-polyacrylamide gel electrophoresis (PAGE) (biotinylation control), and the rest of the lysates were immunoprecipitated using the NiV-specific antiserum gp3 and 40 μl of a suspension of protein A-Sepharose CL-4B (Sigma). Precipitates were washed and were finally suspended in reducing (G protein) or nonreducing (F protein) sample buffer. Following separation on a 10% SDS gel, proteins were transferred to nitrocellulose membranes, and biotinylated proteins were detected with a streptavidin–biotinylated horseradish peroxidase complex (Amersham Pharmacia Biotech) and enhanced chemiluminescence (Thermo Scientific).

Fusion assays. To monitor cell-to-cell fusion for nonpolarized cells, MDCK cells stably expressing NiV wild-type F (Fwt) were seeded onto coverslips at a low density. Twenty-four hours later, cells were transfected with plasmids encoding either wild-type or mutant NiV G. Cell fusion was analyzed at 24 h posttransfection (p.t.) by immunostaining with the G-specific monoclonal antibody mab26 and Alexa Fluor 568-conjugated secondary antibodies. To visualize cell nuclei, cells were subsequently incubated with 4′,6-diamidino-2-phenylindole (DAPI). For fusion assays with polarized cells, MDCK cells stably expressing Fwt protein were seeded onto filter supports and were cultivated for 5 days. Since transfection of polarized cells is enhanced by a short treatment with trypsin or EDTA (14), 0.05% trypsin in 0.53 mM EDTA (Invitrogen) was added to the apical and basal chambers for 10 min to loosen the cell junctions. Then MEM containing 10% FCS was added to inactivate trypsin. Subsequently, transfections with plasmids encoding either wild-type or mutant NiV G proteins were performed using Lipofectamine 2000. Cell fusion was monitored by immunostaining at 48 h after transfection with the G-specific monoclonal antibody (mab26), and cell junctions were visualized by E-cadherin staining as described above. Images were analyzed by confocal laser scanning microscopy (LSM510; Zeiss).

RESULTS

NiV infection causes focus formation in polarized MDCK cells. Epithelial cells represent important target cells in the course of a NiV infection, and virus-positive epithelial cells in the lung and kidney have been detected by immunohistochemistry *in vivo* (for a review, see reference 26). To study NiV infections in cell culture, we used MDCK cells, a well-estab-

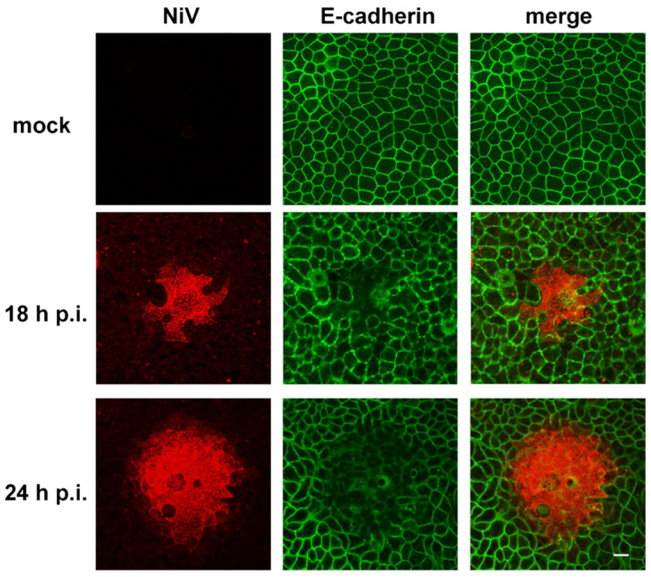

FIG. 1. NiV infection of polarized MDCK cells. MDCK cells were grown on filter supports until full polarization was reached. Then cells either were left uninfected (mock) or were infected with NiV. At 18 h p.i. or 24 h p.i., cells were fixed with 4% PFA for 48 h. Subsequently, cells were stained with a NiV-specific guinea pig antiserum and Alexa Fluor 568-conjugated secondary antibodies. After permeabilization with methanol-acetone, cell junctions were visualized with a monoclonal antibody directed against E-cadherin and with Alexa Fluor 488-conjugated secondary antibodies. Magnification, ×630. Bar, 10 μm.

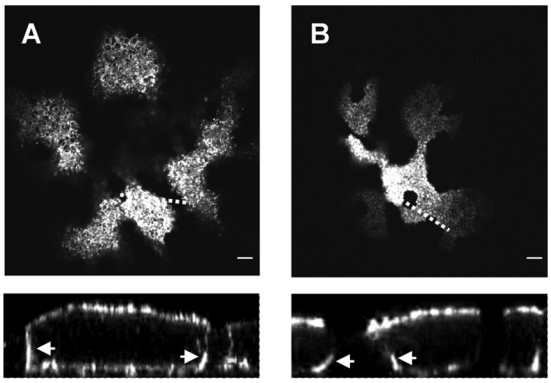

FIG. 2. Distribution of F and G proteins in NiV-induced foci. MDCK cells were cultured on filter supports for 7 days and were then infected with NiV. At 18 h p.i., cells were fixed with 4% PFA for 48 h and were then incubated from the apical and basolateral sides with either F-specific (A) or G-specific (B) monoclonal antibodies and Alexa Fluor 568-conjugated secondary antibodies. (Top) Confocal horizontal (xy) sections through the apical part of the cell monolayer. Dashed lines indicate the lines along which vertical sections were recorded. (Bottom) Vertical (xz) sections through the foci. Arrows indicate lateral membranes. Bars, 10 μm.

lished model epithelial cell line derived from a canine kidney (7, 39). First, we wanted to determine if NiV infects and spreads within these epithelia. Therefore, polarized MDCK cells were grown on filter supports and were infected with NiV from the apical side. At 18 h and 24 h p.i., the samples were inactivated with 4% PFA for 48 h. Virus-positive cells were immunostained with a polyclonal anti-NiV antiserum and Alexa Fluor 568-conjugated secondary antibodies. To visualize cell junctions, cells were permeabilized and E-cadherin was costained with a specific monoclonal antibody and an Alexa Fluor 488-conjugated secondary antibody. As shown in Fig. 1, MDCK cells were readily permissive for NiV. Infection progressed with expanding focus formation in the polarized cell monolayer; the average size of NiV-positive foci was about 20 cells at 18 h p.i. and increased to about 50 cells by 24 h p.i. The formation of foci clearly demonstrates that NiV infection can spread from cell to cell either by virus release and subsequent infection of neighboring cells or by spread across the lateral junctions of epithelial cells. The fact that we never found single NiV-infected cells, even at earlier time points (8 to 16 h p.i.), indicates a relatively rapid spread of virus infection to neighboring cells, definitely faster than we can detect NiV glycoproteins by surface immunostaining. The lack of E-cadherin staining in the centers of NiV-induced foci further demonstrates a disruption of cell junctions between neighboring infected cells (Fig. 1). This might be a result of virus replication *per se*, or it might be due to the expression of specific structural or nonstructural viral proteins, as has been shown for several enveloped and nonenveloped viruses (2, 21, 23, 33). However, disintegration of cell junctions could also be due to direct fusion of adjacent lateral cell membranes induced by the NiV surface glycoproteins. Since both proteins, NiV F and G, are required to mediate fusion (6, 44), this would mean that both glycoproteins are expressed at the lateral membranes of polarized cells.

NiV glycoproteins are expressed at the lateral membranes of infected cells adjacent to noninfected cells. To evaluate the idea of NiV spread and focus formation by glycoprotein-mediated cell-to-cell fusion, the distribution of the NiV glycoproteins on the surfaces of infected polarized epithelial cells was analyzed. Filter-grown MDCK cells were infected with NiV and were immunostained from the apical and the basolateral side with either F- or G-specific monoclonal antibodies. Confocal horizontal sections through the apical part of NiV-positive foci showed pronounced staining for the F (Fig. 2A) and G (Fig. 2B) proteins. However, vertical sections revealed that the glycoprotein localization was not exclusively apical. Substantial amounts were also expressed at the basolateral membranes, indicating bipolar expression of the proteins (Fig. 2, lower panels). In agreement with the lack of E-cadherin staining, demonstrating disruption of lateral membranes in the centers of infection foci (Fig. 1), F and G proteins were found only at lateral membranes at the expanding edges of foci, where infected cells were in contact with yet uninfected cells (Fig. 2, arrows in lower panels). These findings support the model that virus spread and disruption of cell junctions in polarized cell monolayers are the direct results of NiV glycoprotein-mediated cell-to-cell fusion of lateral membranes. The fact that we could not detect cell-free viruses before 16 h p.i. (Fig. 3A), whereas NiV-induced syncytia with more than 5 nuclei were already found at 13 h p.i. (Fig. 3B), further strengthens the idea of a rapid cell-associated spread of infection before dissemination via release of virus particles and reinfection of new target cells.

Both NiV glycoproteins are expressed predominantly on the basolateral surfaces of polarized epithelial cells upon single expression. Since expression of the NiV glycoproteins at baso-

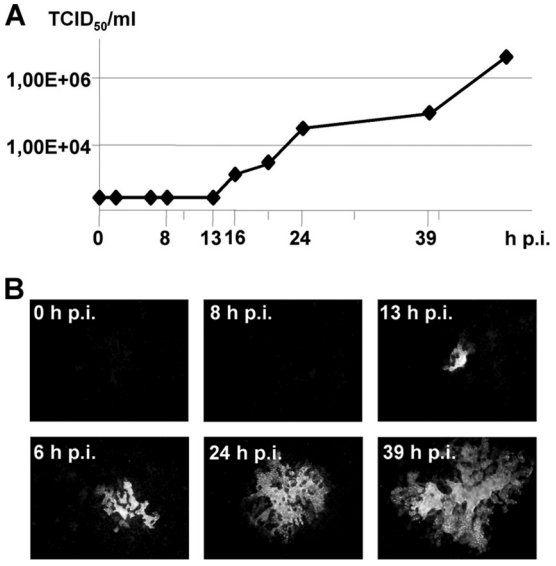

FIG. 3. NiV release and syncytium formation at different time points p.i. MDCK cells were cultivated on filter supports until full polarization was reached. Then cells were infected with NiV at a multiplicity of infection of 10. (A) Virus titers in the supernatants were determined by the $TCID_{50}$ method at 0, 2, 6, 8, 13, 16, 20, 24, 39, and 48 h p.i. (B) To visualize syncytium formation at the indicated time points p.i., cells were fixed, permeabilized with methanol-acetone, and inactivated with 4% PFA. Subsequently, cells were stained with a NiV-specific guinea pig antiserum and Alexa Fluor 568-conjugated secondary antibodies. Magnification, ×200.

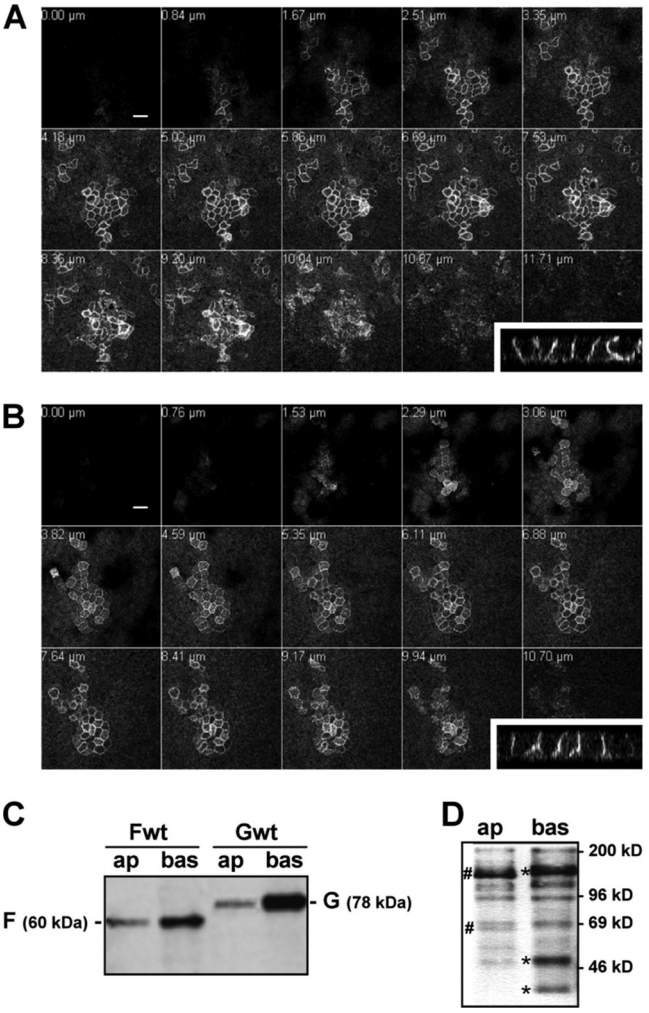

FIG. 4. Surface distribution of wild-type F and G proteins in polarized MDCK cells. (A and B) At 7 days after seeding on filter supports, MDCK cells stably expressing either NiV Fwt (A) or NiV Gwt (B) were incubated with a NiV-specific antiserum from the apical and basolateral sides without prior fixation. Surface-bound antibodies were detected with Alexa Fluor 568-conjugated secondary antibodies. Confocal horizontal sections from top (upper left) to bottom (lower right) are shown. (Insets) Vertical sections. Bars, 20 μm. (C and D) Cell surface proteins were labeled with S-NHS biotin from either the apical (ap) or the basolateral (bas) side. (C) After cell lysis, F and G proteins were immunoprecipitated with NiV-specific antibodies. Precipitates were analyzed by SDS-PAGE under nonreducing (Fwt) or reducing (Gwt) conditions, transferred to nitrocellulose membranes, and probed with peroxidase-conjugated streptavidin. (D) To control surface-selective biotinylation after apical and basolateral labeling, 0.5% of the total-cell lysates was directly subjected to SDS-PAGE, blotting, and streptavidin detection. #, proteins selectively expressed on the apical surface; ∗, proteins found predominantly after basolateral biotinylation.

lateral membranes is a prerequisite for cell-to-cell fusion, we wanted to investigate if the two NiV glycoproteins possess intrinsic sorting signals that ensure basolateral targeting. To study the transport of the NiV glycoproteins in polarized epithelial cells in the absence of other viral proteins and virus-induced cytopathic effects, we generated MDCK cells stably expressing either the NiV F protein or the NiV G protein as described in Materials and Methods. MDCK clones stably expressing F or G were then seeded onto filter supports, and the surface distribution of the viral glycoproteins was analyzed. At 7 days postseeding, apical and basolateral cell surfaces were incubated with a polyclonal anti-NiV antiserum without prior fixation, followed by staining with Alexa Fluor 568-conjugated secondary antibodies. As shown in the confocal analysis of the distribution of the F (Fig. 4A) and G (Fig. 4B) proteins, fluorescent signals for both NiV surface glycoproteins were detected in central and basal but not in apical horizontal sections. In agreement, a cup-like pattern typical for basolateral proteins was observed in the side views (vertical sections shown in insets in Fig. 4A and B).

To confirm the basolateral expression of the F and G proteins by a more quantitative method, we performed selective surface biotinylation. For this purpose, MDCK cell surface proteins of the apical or basolateral domain were labeled by addition of the non-membrane-permeating reagent S-NHS biotin to the respective filter chamber. After cell lysis and immunoprecipitation, F and G proteins were separated by SDS-PAGE and transferred to nitrocellulose membranes. Biotinylated NiV glycoproteins were then detected with peroxidase-conjugated streptavidin. As shown in Fig. 4C, efficient biotinylation of F and G proteins was achieved only after the cells were labeled from the basolateral sides. Less than 10% of the proteins were found to be expressed apically, strongly supporting the idea of targeted basolateral sorting of both NiV glycoproteins. Since we have found that surface-expressed NiV glycoproteins represent 15 to 20% of the total G protein and 8 to 15% of the total F protein (data not shown), we conclude

that less than 2% of the total G protein and less than 1.5% of the total F protein is transported to the apical plasma membrane. To ensure that apical and basolateral surface proteins were labeled selectively in this experiment, total-cell lysates were subjected to SDS-PAGE, Western blotting, and streptavidin detection directly after labeling (biotinylation control). The different quantities of biotin-labeled proteins, and the presence of different protein bands, in apically and basolaterally labeled lysates confirmed that biotinylation is surface specific (Fig. 4D).

Basolateral transport of the NiV glycoproteins is mediated by tyrosine-dependent sorting signals. Basolateral sorting information is frequently encoded in the cytoplasmic tail of transmembrane proteins in the form of small peptide motifs that are recognized by cytosolic adaptor proteins (AP) (4). Most of these sorting motifs are either tyrosine-dependent motifs, conforming to the consensus sequence YxxØ (where Y is a tyrosine, x is any amino acid, and Ø is a bulky hydrophobic amino acid), or dileucine-based motifs (27). The 28-residue cytoplasmic domain of the NiV F protein contains three tyrosines: one at position 525 (Y_{525}) within a YxxØ consensus motif and two adjacent tyrosines at positions 542 and 543. Y_{525} was previously shown to be required for clathrin-mediated endocytosis and hence for proteolytic activation of the F protein by endosomal cathepsins, whereas tyrosines 542 and 543 were not involved in F internalization or cleavage (12, 45). The 45-residue cytoplasmic domain of the NiV G protein contains a membrane-proximal dileucine motif at positions 41 and 42 and also two adjacent tyrosines at positions 28 and 29. Mutation of these amino acids ($Y_{28/29}$; $L_{41/42}$) affected neither the endocytosis nor the fusion helper function of the G protein (45). To elucidate if the tyrosines and the dileucine-based motif in the cytoplasmic portions of F and G represent basolateral targeting signals, mutant glycoproteins in which the critical tyrosines or leucines were replaced by alanines (Fig. 5A) were generated and stably expressed in MDCK cells. The surface distribution of the mutants was analyzed by confocal microscopy. As shown in Fig. 5B, mutation of Y_{525} in the YxxØ motif resulted in an apical redistribution of the F protein, whereas mutation of the two tyrosines ($F_{Y542/543A}$) did not alter the basolateral expression of the F protein. Surprisingly, mutation of the dileucine motif in the cytoplasmic tail of the G protein, which we would have predicted to function as a basolateral targeting signal, had no effect on polarized G distribution (Fig. 5C, $G_{L41/42A}$). In contrast, polarized sorting was affected by mutation of the two adjacent tyrosines. Mutant $G_{Y28/29A}$ was clearly expressed apically (Fig. 5C). The finding that G proteins with single tyrosine mutations were also localized at apical cell surfaces (Fig. 5C, G_{Y28A} and G_{Y29A}) clearly indicates that within the dityrosine motif, both residues are required for correct basolateral sorting.

Apical retargeting of the G protein prevents syncytium formation in polarized MDCK cells. To investigate the significance of basolateral sorting of glycoproteins F and G for NiV-mediated cell-to-cell fusion in epithelia, wild-type and mutant F and G proteins were coexpressed in nonpolarized and polarized MDCK cells. Because apically retargeted F_{Y525A} is endocytosis deficient and consequently is not cleaved and is fusion inactive (45; C. Weise, unpublished observation), the fusion activities of coexpressed apical mutant F and basolateral

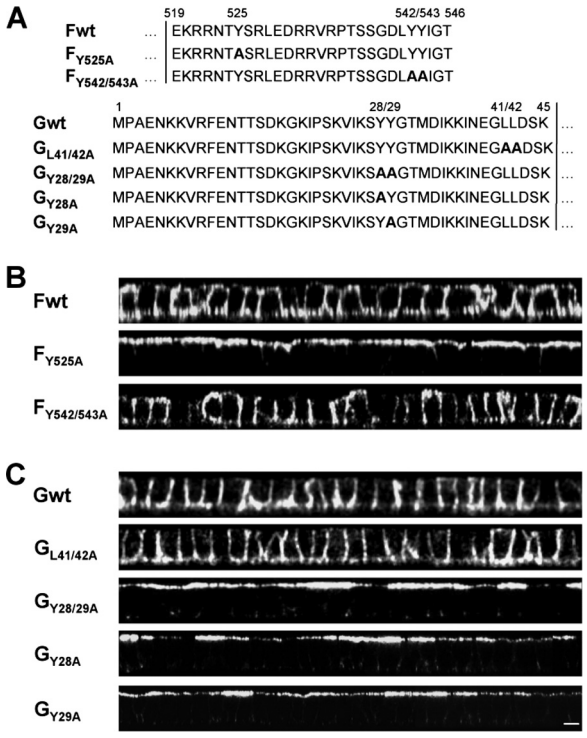

FIG. 5. Surface distribution of mutant F and G proteins. (A) Amino acid sequences of the cytoplasmic domains of wild-type and mutant F and G proteins. Numbers above the sequences indicate amino acid positions. Boldface letters indicate exchanged amino acid residues. Vertical lines indicate the beginning of the predicted transmembrane domains. (B and C) Surface distribution of mutant NiV glycoproteins. MDCK cells stably expressing either wild-type or mutant NiV F (B) or G (C) proteins were immunostained as described in the legend to Fig. 4. Vertical sections through the cell monolayers are shown. Bar, 10 μm.

G proteins cannot be tested. We thus analyzed fusion in cells expressing basolateral Fwt in combination with either basolaterally expressed G proteins (Gwt and $G_{L41/42A}$) or apically targeted $G_{Y28/29A}$. To ensure coexpression of the F and G proteins in one cell, we transfected an MDCK cell clone that stably expressed Fwt protein at basolateral surfaces in 100% of the cells with different G plasmids. For fusion assays in nonpolarized cells, cells were grown on coverslips to 70% confluence. For fusion assays in polarized cells, cells were cultivated on filter supports until polarization was reached. Nonpolarized and polarized F-expressing MDCK cells were then transfected with plasmids encoding either wild-type or mutant G proteins as described in Materials and Methods. At 24 h (nonpolarized cells) or 48 h (polarized cells) p.t., G-positive cells were detected with G-specific antibodies. As shown in Fig. 6A, all G proteins—Gwt, $G_{L41/42A}$, and $G_{Y28/29A}$—induced the formation of large syncytia in nonpolarized F-expressing MDCK cells, confirming that all G proteins were expressed at similar levels and were biologically active. In contrast to nonpolarized cells, fusion of polarized cells was observed only when cells were transfected with Gwt or $G_{L41/42A}$ (Fig. 6B, Fwt + Gwt and Fwt + $G_{L41/42A}$). In polarized cells transfected with $G_{Y28/29A}$, G protein was apically expressed, and only single G-positive cells could be detected (Fig. 6B, Fwt + $G_{Y28/29A}$).

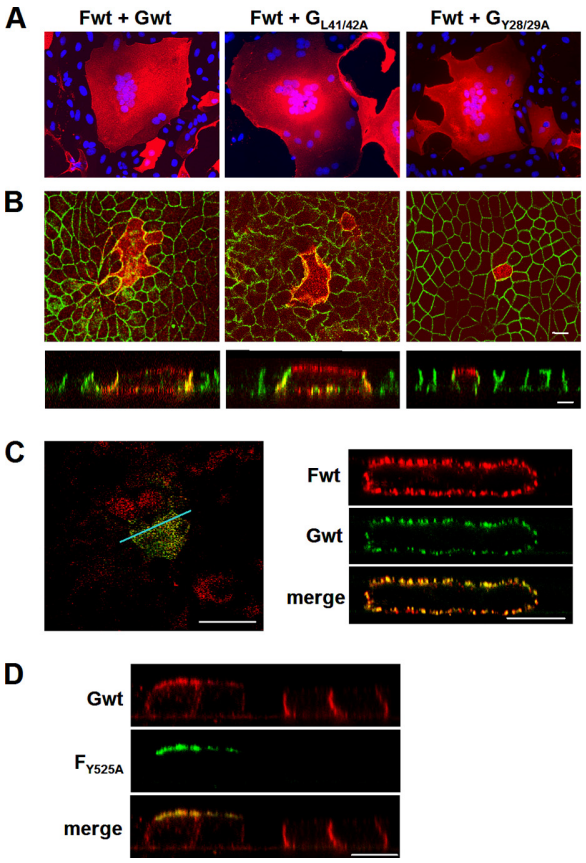

FIG. 6. Fusion activity and surface distribution of wild-type and mutant NiV F and G proteins upon coexpression. (A) Syncytium formation in nonpolarized MDCK cells. Subconfluent MDCK cells stably expressing NiV Fwt were transfected with plasmids encoding either Gwt protein (Fwt + Gwt) or a mutant NiV G protein (Fwt + $G_{L41/42A}$ or Fwt + $G_{Y28/29A}$). At 24 h p.t., syncytia were visualized by staining with a G-specific monoclonal antibody without prior fixation, and the primary antibody was detected with Alexa Fluor 568-conjugated secondary antibodies. Cell nuclei were counterstained with DAPI. Magnification, ×200. (B) Syncytium formation in polarized MDCK cells. MDCK cells stably expressing NiV F protein were grown on filter supports. At 5 days postseeding, cells were transfected with plasmids encoding either wild-type or mutant NiV G. G-positive cells were stained at 48 h p.t. as described above. After permeabilization, cell junctions were visualized with an E-cadherin-specific monoclonal antibody and Alexa Fluor 488-conjugated secondary antibodies. Confocal horizontal sections (top) and side views (bottom) are shown. (C) Distribution of wild-type F and G proteins in polarized MDCK cells upon coexpression. MDCK cells stably expressing Fwt were grown on filter supports until full polarization was reached. Then the cells were transfected with a plasmid encoding Gwt. At 48 h p.t., stably expressed Fwt was surface stained from both sides with F-specific monoclonal antibodies and Alexa Fluor 568-conjugated secondary antibodies. The transiently expressed Gwt was then detected with G-specific antibodies and Alexa Fluor 488-conjugated secondary antibodies. (Left) Confocal xy section through the apical part of the monolayer; (right) vertical section recorded along the line indicated by the blue line in the right panel. (D) Distribution of wild-type G protein upon coexpression with F_{Y525A}. Polarized Gwt-expressing MDCK cells were transfected with mutant F_{Y525A}. At 48 h p.t., Gwt was surface stained from both sides with G-specific monoclonal antibodies and Alexa Fluor 568-conjugated secondary antibodies. The transiently expressed F_{Y525A} was then detected with F-specific antibodies and Alexa Fluor 488-conjugated secondary antibodies. Confocal vertical sections are shown. Bars, 10 μm.

In agreement with the idea that fusogenic proteins must be expressed on the basolateral cell surface to induce fusion (40), apically expressed G proteins were unable to mediate fusion. We thus conclude that inactivation of the basolateral targeting signal, leading to apical retargeting of one of the NiV glycoproteins, prevents cell-to-cell fusion in polarized cell cultures.

The vertical sections through the syncytia shown in the lower panels of Fig. 6B revealed that Gwt and $G_{L41/42A,}$ which were found to be expressed almost exclusively on the basolateral cell surface upon single expression (Fig. 5C), were expressed both basolaterally and apically when coexpressed with the F protein. To determine if the F protein is also redistributed upon coexpression with the G protein, costaining of F and G proteins was performed. Figure 6C clearly shows a bipolar distribution and colocalization of the F and the G wild-type proteins. As in the foci of NiV-infected cells (Fig. 2), coexpressed F and G proteins in syncytia were not predominantly found basolaterally. This suggests that after cell-to-cell fusion, bipolar redistribution is not due to other viral factors (e.g., the matrix protein) but rather results from NiV glycoprotein-induced cell-to-cell fusion in infected or in transfected cells, which disrupts the integrity and polarity of the epithelial cells, leading to missorting of both glycoproteins to the apical cell surface. As a consequence, lateral glycoprotein expression is only transiently observed at the edges of syncytia and is lost as soon as the infected cells become an integral part of the syncytia. Finally, to determine if the NiV glycoproteins can influence their distribution mutually in epithelia with intact polarity, and thus in the absence of fusion, cells stably expressing Gwt were transfected with the apically retargeted mutant F_{Y525A}, which is not cleaved and is fusion incompetent. The costaining of the two NiV glycoproteins shown in Fig. 6D demonstrates that in cells expressing only Gwt, the protein was almost exclusively expressed basolaterally, as observed before (see Fig. 4B). However, in cells coexpressing F_{Y525A}, Gwt was clearly retargeted to the apical cell surface. Interestingly, F_{Y525A} was not redirected to the basolateral membrane. The finding that apical F leads to apical retargeting of G, whereas basolateral G does not redirect apical F to basolateral surfaces, suggests that both proteins form complexes that are cosorted according to the targeting information in the F protein. However, even if cosorting of G is observed in the absence of fusion events, distribution in virus-infected cells is most likely influenced primarily by the disruption of integrity and cell polarity due to cell-to-cell fusion.

DISCUSSION

Our data provide conclusive evidence that both NiV glycoproteins possess tyrosine-dependent targeting signals in their cytoplasmic domains that are required for basolateral sorting in polarized epithelial cells. Disruption of the signals leads to apical retargeting and prevents cell-to-cell fusion in polarized cell monolayers, demonstrating the functional importance of basolateral F and G expression for NiV spread in epithelia.

In polarized cells, intrinsic protein-sorting codes are recognized and segregated by cytoplasmic adaptor complexes that regulate protein trafficking. This sorting can be achieved through the delivery of newly synthesized membrane proteins to the appropriate domains of the plasma membrane or

through indirect pathways involving the selective stabilization or redistribution of cell surface proteins (28). Since interaction with cytosolic adaptor proteins (AP) leads to the selective recruitment of cargo proteins into either endosomes or lysosomes or to the basolateral cell membrane (4, 19), endocytosis and basolateral sorting signals often overlap (5). This is clearly true for Y_{525} in the YSRL motif in the F protein, which we have previously shown to function as a signal for clathrin-mediated endocytosis (45), and which was identified as a basolateral targeting signal in this study. Even if it is not entirely clear which apical and basolateral proteins travel from the Golgi apparatus to the plasma membrane by direct pathways, which proteins reach the surface via endosomes, and which proteins use a transcytotic mode of delivery (39), it can be assumed that the μ subunit of AP-2 recognizes the YxxØ motif, resulting in NiV F protein clustering in clathrin-coated pits. In endosomes, the YSRL signal in the F protein is likely recognized by the AP-1–clathrin complex, and the protein is recycled back to the plasma membrane. In polarized epithelia, AP-1B is likely responsible for transport to the basolateral cell surface via basolateral or common recycling endosomes (18; for a review, see reference 16).

Unexpectedly, basolateral transport of the G protein did not depend on the dileucine motif, a signal shown to act as a targeting signal in other proteins with basolateral expression (1, 20, 22, 25). Instead of the dileucine signal, a dityrosine motif is responsible for basolateral G targeting. To our knowledge, NiV G is the first protein in which two adjacent tyrosines are responsible for basolateral sorting. The finding that the two tyrosines at positions 542 and 543 in the NiV F protein do not act as a functional basolateral targeting signal suggests that the dityrosine motif in the G protein requires additional sequence- or conformation-related information in the cytoplasmic tail to be recognized as a sorting signal. It will be the aim of future studies to define these requirements. Furthermore, the question of whether the recruitment of G into basolateral transport vesicles depends on AP-1B or AP-4, the only AP complexes identified to date that are definitively associated with basolateral protein trafficking (17, 43; for a review, see reference 28), has to be elucidated. Even though it has recently been proposed that henipavirus F and G proteins associate only after trafficking to the cell surface (46), we have some evidence that G protein sorting can be influenced by the NiV F protein (Fig. 6D). It thus remains to be determined to what extent F-G complex formation or interactions with other viral proteins affect the dityrosine-based intracellular transport and sorting of the G protein.

Mucosal surfaces in the respiratory tract are composed primarily of polarized epithelial cells but also contain specialized cells, such as mucus-secreting goblet cells and M cells, as part of the mucosal lymphoid organs (42, 47). Many microorganisms have evolved mechanisms to gain access to the blood circulation after entering the respiratory tract. However, the pathways used to cross the mucosal barriers of the lungs can differ significantly. For example, reoviruses have been shown to enter through intestinal as well as pulmonary M cells and subsequently to spread to regional lymph nodes (32, 48). For arenaviruses, it was recently speculated that entry into the respiratory tract likely occurs when epithelial tight-junction permeability and integrity are compromised by injury or disease (15). Also, the prototype member of the *Morbillivirus* genus within the family *Paramyxoviridae*, measles virus (MV), does not directly infect respiratory epithelial cells but is trapped by dendritic cells via attachment to the C-type lectin DC-SIGN (dendritic-cell-specific intercellular adhesion molecule 3-grabbing nonintegrin) and is subsequently transported to the local lymph system, in which the major target cells, namely, lymphocytes and macrophages, are then productively infected (10, 11). In contrast to MV, NiV seldom infects lymphocytes and macrophages, since the main target cells of systemic NiV infection are endothelial and smooth muscle cells (for a review, see reference 26 and references therein). Thus, it is highly unlikely that NiV enters the body via dendritic cells in the respiratory tract and subsequently infects immune cells, which then disseminate the virus systemically. NiV rather overcomes the epithelial barrier by directly infecting respiratory epithelial cells, with subsequent spread to underlying tissue and dissemination via the blood system. The results of this study suggest that NiV glycoprotein-mediated cell-to-cell fusion in the airway mucosa supports the establishment of the primary infection not only by promoting the spread of infection at the virus entry site but also by disrupting the epithelial barrier in the respiratory tract, facilitating virus entry into subepithelial tissues. In addition to playing an important role in early infection phases, the direct spread of infection across lateral membranes of polarized cells probably plays a crucial role in late stages of infection. After systemic dissemination and productive infection of many organs, efficient cell-to-cell spread in epithelia likely contributes to widespread infection in mucosal surfaces of the respiratory or urinary tract, thus promoting the production of infected material (NiV-infected cells or cell-free viruses), which is then shed via saliva and urine and can transmit the infection to other susceptible hosts.

ACKNOWLEDGMENTS

We thank Benhur Lee, UCLA, Los Angeles, CA, and Heinz Feldmann, NIH, Hamilton, MT, for kindly providing NiV-specific antibodies. We gratefully acknowledge Gunther Doehlemann, MPI, Marburg, Germany, for supporting the confocal microscopy studies. We also thank Gert Zimmer, Larissa Kolesnikova, Hans-Dieter Klenk, and Stephan Becker for helpful suggestions on the manuscript.

This work was supported by grants from the German Research Foundation (DFG) to A.M. (GK 1216 and SFB 593/TP B11).

REFERENCES

1. **Bello, V., J. W. Goding, V. Greengrass, A. Sali, V. Dubljevic, C. Lenoir, G. Trugnan, and M. Maurice.** 2001. Characterization of a di-leucine-based signal in the cytoplasmic tail of the nucleotide-pyrophosphatase NPP1 that mediates basolateral targeting but not endocytosis. Mol. Biol. Cell **12:**3004–3015.
2. **Benedicto, I., F. Molina-Jimenez, O. Barreiro, A. Maldonado-Rodriguez, J. Prieto, R. Moreno-Otero, R. Aldabe, M. Lopez-Cabrera, and P. L. Majano.** 2008. Hepatitis C virus envelope components alter localization of hepatocyte tight junction-associated proteins and promote occludin retention in the endoplasmic reticulum. Hepatology **48:**1044–1053.
3. **Bonaparte, M. I., A. S. Dimitrov, K. N. Bossart, G. Crameri, B. A. Mungall, K. A. Bishop, V. Choudhry, D. S. Dimitrov, L. F. Wang, B. T. Eaton, and C. C. Broder.** 2005. Ephrin-B2 ligand is a functional receptor for Hendra virus and Nipah virus. Proc. Natl. Acad. Sci. U. S. A. **102:**10652–10657.
4. **Bonifacino, J. S., and E. C. Dell'Angelica.** 1999. Molecular bases for the recognition of tyrosine-based sorting signals. J. Cell Biol. **145:**923–926.
5. **Bonifacino, J. S., and L. M. Traub.** 2003. Signals for sorting of transmembrane proteins to endosomes and lysosomes. Annu. Rev. Biochem. **72:**395–447.
6. **Bossart, K. N., L. F. Wang, M. N. Flora, K. B. Chua, S. K. Lam, B. T. Eaton, and C. C. Broder.** 2002. Membrane fusion tropism and heterotypic functional activities of the Nipah virus and Hendra virus envelope glycoproteins. J. Virol. **76:**11186–11198.

7. **Cereijido, M., E. S. Robbins, W. J. Dolan, C. A. Rotunno, and D. D. Sabatini.** 1978. Polarized monolayers formed by epithelial cells on a permeable and translucent support. J. Cell Biol. **77:**853–880.
8. **Chua, K. B., W. J. Bellini, P. A. Rota, B. H. Harcourt, A. Tamin, S. K. Lam, T. G. Ksiazek, P. E. Rollin, S. R. Zaki, W. Shieh, C. S. Goldsmith, D. J. Gubler, J. T. Roehrig, B. Eaton, A. R. Gould, J. Olson, H. Field, P. Daniels, A. E. Ling, C. J. Peters, L. J. Anderson, and B. W. Mahy.** 2000. Nipah virus: a recently emergent deadly paramyxovirus. Science **288:**1432–1435.
9. **Chua, K. B., K. J. Goh, K. T. Wong, A. Kamarulzaman, P. S. Tan, T. G. Ksiazek, S. R. Zaki, G. Paul, S. K. Lam, and C. T. Tan.** 1999. Fatal encephalitis due to Nipah virus among pig-farmers in Malaysia. Lancet **354:**1257–1259.
10. **de Swart, R. L.** 2008. The pathogenesis of measles revisited. Pediatr. Infect. Dis. J. **27:**S84–S88.
11. **de Witte, L., M. Abt, S. Schneider-Schaulies, Y. van Kooyk, and T. B. Geijtenbeek.** 2006. Measles virus targets DC-SIGN to enhance dendritic cell infection. J. Virol. **80:**3477–3486.
12. **Diederich, S., M. Moll, H. D. Klenk, and A. Maisner.** 2005. The Nipah virus fusion protein is cleaved within the endosomal compartment. J. Biol. Chem. **280:**29899–29903.
13. **Diederich, S., L. Thiel, and A. Maisner.** 2008. Role of endocytosis and cathepsin-mediated activation in Nipah virus entry. Virology **375:**391–400.
14. **Düchler, M., M. Pengg, S. Brunner, M. Muller, G. Brem, and E. Wagner.** 2001. Transfection of epithelial cells is enhanced by combined treatment with mannitol and polyethylene glycol. J. Gene Med. **3:**115–124.
15. **Dylla, D. E., D. E. Michele, K. P. Campbell, and P. B. McCray, Jr.** 2008. Basolateral entry and release of New and Old World arenaviruses from human airway epithelia. J. Virol. **82:**6034–6038.
16. **Fölsch, H., P. E. Mattila, and O. A. Weisz.** 2009. Taking the scenic route: biosynthetic traffic to the plasma membrane in polarized epithelial cells. Traffic **10:**972–981.
17. **Fölsch, H., H. Ohno, J. S. Bonifacino, and I. Mellman.** 1999. A novel clathrin adaptor complex mediates basolateral targeting in polarized epithelial cells. Cell **99:**189–198.
18. **Gan, Y., T. E. McGraw, and E. Rodriguez-Boulan.** 2002. The epithelial-specific adaptor AP1B mediates post-endocytic recycling to the basolateral membrane. Nat. Cell Biol. **4:**605–609.
19. **Gravotta, D., A. Deora, E. Perret, C. Oyanadel, A. Soza, R. Schreiner, A. Gonzalez, and E. Rodriguez-Boulan.** 2007. AP1B sorts basolateral proteins in recycling and biosynthetic routes of MDCK cells. Proc. Natl. Acad. Sci. U. S. A. **104:**1564–1569.
20. **Hunziker, W., and C. Fumey.** 1994. A di-leucine motif mediates endocytosis and basolateral sorting of macrophage IgG Fc receptors in MDCK cells. EMBO J. **13:**2963–2969.
21. **Javier, R. T.** 2008. Cell polarity proteins: common targets for tumorigenic human viruses. Oncogene **27:**7031–7046.
22. **Jespersen, T., H. B. Rasmussen, M. Grunnet, H. S. Jensen, K. Angelo, D. S. Dupuis, L. K. Vogel, N. K. Jorgensen, D. A. Klaerke, and S. P. Olesen.** 2004. Basolateral localisation of KCNQ1 potassium channels in MDCK cells: molecular identification of an N-terminal targeting motif. J. Cell Sci. **117:**4517–4526.
23. **Lara-Pezzi, E., S. Roche, O. M. Andrisani, F. Sanchez-Madrid, and M. Lopez-Cabrera.** 2001. The hepatitis B virus HBx protein induces adherens junction disruption in a src-dependent manner. Oncogene **20:**3323–3331.
24. **Luby, S. P., M. J. Hossain, E. S. Gurley, B. N. Ahmed, S. Banu, S. U. Khan, N. Homaira, P. A. Rota, P. E. Rollin, J. A. Comer, E. Kenah, T. G. Ksiazek, and M. Rahman.** 2009. Recurrent zoonotic transmission of Nipah virus into humans, Bangladesh, 2001–2007. Emerg. Infect. Dis. **15:**1229–1235.
25. **Madrid, R., S. Le Maout, M. B. Barrault, K. Janvier, S. Benichou, and J. Merot.** 2001. Polarized trafficking and surface expression of the AQP4 water channel are coordinated by serial and regulated interactions with different clathrin-adaptor complexes. EMBO J. **20:**7008–7021.
26. **Maisner, A., J. Neufeld, and H. Weingartl.** 2009. Organ- and endotheliotropism of Nipah virus infections in vivo and in vitro. Thromb. Haemost. **102:**1014–1023.
27. **Marks, M. S., L. Woodruff, H. Ohno, and J. S. Bonifacino.** 1996. Protein targeting by tyrosine- and di-leucine-based signals: evidence for distinct saturable components. J. Cell Biol. **135:**341–354.
28. **Mellman, I., and W. J. Nelson.** 2008. Coordinated protein sorting, targeting and distribution in polarized cells. Nat. Rev. Mol. Cell Biol. **9:**833–845.
29. **Middleton, D. J., H. A. Westbury, C. J. Morrissy, B. M. van der Heide, G. M. Russell, M. A. Braun, and A. D. Hyatt.** 2002. Experimental Nipah virus infection in pigs and cats. J. Comp. Pathol. **126:**124–136.
30. **Mohd Nor, M. N., C. H. Gan, and B. L. Ong.** 2000. Nipah virus infection of pigs in peninsular Malaysia. Rev. Sci. Tech. **19:**160–165.
31. **Moll, M., S. Diederich, H. D. Klenk, M. Czub, and A. Maisner.** 2004. Ubiquitous activation of the Nipah virus fusion protein does not require a basic amino acid at the cleavage site. J. Virol. **78:**9705–9712.
32. **Morin, M. J., A. Warner, and B. N. Fields.** 1996. Reovirus infection in rat lungs as a model to study the pathogenesis of viral pneumonia. J. Virol. **70:**541–548.
33. **Moser, L. A., M. Carter, and S. Schultz-Cherry.** 2007. Astrovirus increases epithelial barrier permeability independently of viral replication. J. Virol. **81:**11937–11945.
34. **Mungall, B. A., D. Middleton, G. Crameri, K. Halpin, J. Bingham, B. T. Eaton, and C. C. Broder.** 2007. Vertical transmission and fetal replication of Nipah virus in an experimentally infected cat. J. Infect. Dis. **196:**812–816.
35. **Negrete, O. A., D. Chu, H. C. Aguilar, and B. Lee.** 2007. Single amino acid changes in the Nipah and Hendra virus attachment glycoproteins distinguish ephrinB2 from ephrinB3 usage. J. Virol. **81:**10804–10814.
36. **Negrete, O. A., E. L. Levroney, H. C. Aguilar, A. Bertolotti-Ciarlet, R. Nazarian, S. Tajyar, and B. Lee.** 2005. EphrinB2 is the entry receptor for Nipah virus, an emergent deadly paramyxovirus. Nature **436:**401–405.
37. **Pager, C. T., W. W. Craft, Jr., J. Patch, and R. E. Dutch.** 2006. A mature and fusogenic form of the Nipah virus fusion protein requires proteolytic processing by cathepsin L. Virology **346:**251–257.
38. **Paton, N. I., Y. S. Leo, S. R. Zaki, A. P. Auchus, K. E. Lee, A. E. Ling, S. K. Chew, B. Ang, P. E. Rollin, T. Umapathi, I. Sng, C. C. Lee, E. Lim, and T. G. Ksiazek.** 1999. Outbreak of Nipah-virus infection among abattoir workers in Singapore. Lancet **354:**1253–1256.
39. **Rodriguez-Boulan, E., G. Kreitzer, and A. Musch.** 2005. Organization of vesicular trafficking in epithelia. Nat. Rev. Mol. Cell Biol. **6:**233–247.
40. **Roth, M. G., and R. W. Compans.** 1980. Antibody-resistant spread of vesicular stomatitis virus infection in cell lines of epithelial origin. J. Virol. **35:**547–550.
41. **Runkler, N., E. Dietzel, M. Carsillo, S. Niewiesk, and A. Maisner.** 2009. Sorting signals in the measles virus wild-type glycoproteins differently influence virus spread in polarized epithelia and lymphocytes. J. Gen. Virol. **90:**2474–2482.
42. **Shami, S. G., and M. J. Evans.** 1992. Kinetics of pulmonary cells, p. 145–155. *In* R. A. Parent (ed.), Comparative biology of the normal lung. CRC Press, Boca Raton, FL.
43. **Simmen, T., S. Honing, A. Icking, R. Tikkanen, and W. Hunziker.** 2002. AP-4 binds basolateral signals and participates in basolateral sorting in epithelial MDCK cells. Nat. Cell Biol. **4:**154–159.
44. **Tamin, A., B. H. Harcourt, T. G. Ksiazek, P. E. Rollin, W. J. Bellini, and P. A. Rota.** 2002. Functional properties of the fusion and attachment glycoproteins of Nipah virus. Virology **296:**190–200.
45. **Vogt, C., M. Eickmann, S. Diederich, M. Moll, and A. Maisner.** 2005. Endocytosis of the Nipah virus glycoproteins. J. Virol. **79:**3865–3872.
46. **Whitman, S. D., E. C. Smith, and R. E. Dutch.** 2009. Differential rates of protein folding and cellular trafficking for the Hendra virus F and G proteins: implications for F-G complex formation. J. Virol. **83:**8998–9001.
47. **Wolf, J. L., and W. A. Bye.** 1984. The membranous epithelial (M) cell and the mucosal immune system. Annu. Rev. Med. **35:**95–112.
48. **Wolf, J. L., D. H. Rubin, R. Finberg, R. S. Kauffman, A. H. Sharpe, J. S. Trier, and B. N. Fields.** 1981. Intestinal M cells: a pathway for entry of reovirus into the host. Science **212:**471–472.
49. **Wong, K. T., W. J. Shieh, S. Kumar, K. Norain, W. Abdullah, J. Guarner, C. S. Goldsmith, K. B. Chua, S. K. Lam, C. T. Tan, K. J. Goh, H. T. Chong, R. Jusoh, P. E. Rollin, T. G. Ksiazek, and S. R. Zaki.** 2002. Nipah virus infection: pathology and pathogenesis of an emerging paramyxoviral zoonosis. Am. J. Pathol. **161:**2153–2167.
50. **Yob, J. M., H. Field, A. M. Rashdi, C. Morrissy, B. van der Heide, P. Rota, A. bin Adzhar, J. White, P. Daniels, A. Jamaluddin, and T. Ksiazek.** 2001. Nipah virus infection in bats (order Chiroptera) in peninsular Malaysia. Emerg. Infect. Dis. **7:**439–441.